JOURNAL OF SOLID STATE CHEMISTRY **136,** 46–50 (1998)
ARTICLE NO. SC977649

Synthesis and Structure Determination of $La_8Ti_{10}S_{24}O_4$

L. Cario,[1] C. Deudon, A. Meerschaut, and J. Rouxel

Laboratoire de Chimie des Solides, Institut des Matériaux de Nantes, UMR-CNRS 110, 2 rue de la Houssinière, B.P. 32229, 44322 Nantes Cedex 3, France

Received November 25, 1996; in revised form September 24, 1997; accepted October 7, 1997

The new compound $La_8Ti_{10}S_{24}O_4$ has been prepared from a mixture of $La_2Ti_2O_7$ and La_2O_3 (in a 5:1 ratio) heated at 1200°C under a H_2S gas flow. This new quaternary phase was obtained due to an incomplete sulfidizing process. Single-crystal X-ray diffraction studies show that $La_8Ti_{10}S_{24}O_4$ crystallizes in space group *P4/mmm*, with $Z = 1$, in a cell of dimensions $a = b = 10.421$ Å and $c = 8.384$ Å. Least-squares refinement converged to values of $R = 0.045$ and $R_w = 0.048$. The structure can be viewed as a stacking of two types of layers along the $\vec{c}$ axis. These layers are built up from infinite rutile-like chains (Ti octahedra) that cross perpendicularly. La atoms, in a tricapped prismatic coordination, are located in tunnels that develop parallel to the $\vec{c}$ direction.

INTRODUCTION

Whereas a large number of ternary oxides or sulfides of lanthanides and transition metal elements are known, only a few quaternary oxysulfides have been reported. However, recently, several new La/Ti oxysulfide phases have been discovered, including $La_6Ti_2S_8O_5$ and $La_4Ti_3S_4O_8$ (1), $La_{20}Ti_{11}S_{44}O_6$ (2), and $Sr_{5.8}La_{4.4}Ti_{7.8}S_{24}O_4$ and $La_{14}Ti_8S_{33}O_4$ (3). The last three phases, which have a lower oxygen content than the first two phases, exhibit some common structural features. Indeed, structures of these three phases can be viewed as $^2_\infty[(Ti_4S_2O_4)(TiS_6)(Ti_2S_{10})]$ layers for $La_{20}Ti_{11}S_{44}O_6$ and $^2_\infty[(Ti_4S_2O_4)(TiS_6)(TiS_6)]$ layers for $Sr_{5.8}La_{4.4}Ti_{7.8}S_{24}O_4$ and $La_{14}Ti_8S_{33}O_4$. These layers are built up from rutile-like, edge-sharing chains that cross perpendicularly. Such layers can be designated as 1–2 and 1–1 types, respectively, taking into account the number of isolated Ti-centered octahedra located between each $Ti_4S_2O_4$ cluster along the two directions of the layer plane.

The present structural study of $La_8Ti_{10}S_{24}O_4$ shows that the structure is closely related to that of $Sr_{5.8}La_{4.4}Ti_{7.8}S_{24}O_4$ and is perhaps similar to the all-lanthanum $La_9Ti_9S_{24}O_4$ analog mentioned but not described in ref 3. However, the oxidation state for titanium ions in the $La_8Ti_{10}S_{24}O_4$ compound is different from what is stated for the Sr/La derivative (3). Thus, the presence of Ti^{3+} and Ti^{4+} in $La_8Ti_{10}S_{24}O_4$ is needed to maintain the charge equilibrium between cations (La^{3+}, Ti^{3+}–Ti^{4+}) and anions (S^{2-}, O^{2-}), whereas only Ti^{4+} is needed for charge equilibrium in the Sr/La derivative.

[1]To whom correspondence should be addressed.

PREPARATION

The $La_8Ti_{10}S_{24}O_4$ phase was obtained as a side product from the sulfurization of a mixture of $La_2Ti_2O_7$ and La_2O_3 in 5:1 ratio to get the $(LaS)_{1+x}TiS_2$ misfit compound. The oxide mixture was placed in a graphite crucible and kept under a H_2S gas flow at 1200°C for 7 h. The products of the reaction, with a small amount of iodine for vapor transport, were then sealed in a quartz ampoule under vacuum (2×10^{-2} torr) and heated at 1050°C with a temperature gradient of about 100°C for 1 week. Because of the incomplete sulfurization, a majority of small black $La_8Ti_{10}S_{24}O_4$ crystallites with a truncated parallelepiped shape were obtained in addition to the misfit phase.

Semiquantitative chemical analyses were performed with a JEOL 5800 SEM equipped with a PGT microanalyzer (4). Analyses on several crystals gave a La/Ti/S ratio of 1.07/1.01/3, not the theoretical 1/1.25/3 ratio. The poor agreement is likely related to the overlap of the La (L) and Ti (K) emission lines. The presence of oxygen was detected by this technique but semiquantitative analysis for this element could not be performed.

SYMMETRY AND UNIT CELL PARAMETERS

A powder X-ray diffraction pattern of $La_8Ti_{10}S_{24}O_4$ (selected crystals) is shown in Fig. 1. A least-squares refinement of the unit cell parameters leads to $a = b = 10.4223(8)$ Å and $c = 8.3840(7)$ Å.

Preliminary precession and Weissenberg X-ray investigations indicated a tetragonal symmetry. No observed systematic condition was detected. A suitable crystal ($0.14 \times 0.08 \times 0.09$ mm^3) was mounted on an Enraf-Nonius CAD4 diffractometer for data collection. Unit cell parameters of this crystal were determined from 25 reflections in the range $22.2° < 2\theta < 50.7°$.

0022-4596/98 $25.00

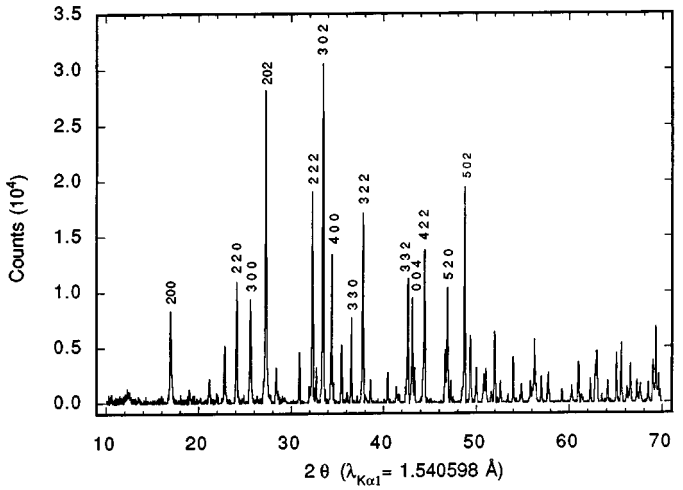

FIG. 1. Powder X-ray diffraction pattern. Indexing is only for $I_{obs} > 20$.

Cell parameters and the experimental conditions for data collection are listed in Table 1. The structure was partially solved by direct methods using the SHELXTL (5) program; refinements were performed with JANA chain programs (6).

STRUCTURE REFINEMENT

A total of 4382 reflections were measured within the range $-16 < h < 16$, $0 < k < 16$, $0 < l < 13$, $1.5° < \theta < 35°$, of which 2922 were above the significance level of $3\sigma(I)$. Crystal stabilities were checked by monitoring the intensities of three standard reflections every hour. No decay was observed during the data collection period. The intensity data were corrected for Lorentz–polarization effects by Sysext (7) and for absorption by XTAL34 (8).

TABLE 1
Details of the Data Collection and Refinement Results for the Structure Determination of $La_8Ti_{10}S_{24}O_4$

$La_8Ti_{10}S_{24}O_4$: formula units/cell $Z = 1$	
Formula weight = 2434.63 g/mol	
Tetragonal symmetry, space group $P4/mmm$ (No. 123)	
$a = 10.4207(9)$ Å, $b = 10.4207(9)$ Å, $c = 8.3838(5)$ Å	
Temperature of measurement (K)	293
Wavelength (Å)	$\lambda(\mathrm{Mo}K\alpha) = 0.7107$
Monochromator	graphite
Calculated density ($g\,cm^{-3}$)	$\rho_{calc} = 4.422$
Absorption coefficient (cm^{-1})	$\mu = 125.64$
θ range (deg)	1.5–35
Scan w: $\Delta w = 1.00 + 0.35 \tan\theta$	
Number of independent reflections ($I \geq 3\sigma(I)$)	924
Number of variables	39
$R = 0.045$, $R_w = 0.048$	
Min transmission coeff	0.1889
Max transmission coeff	0.4017

TABLE 2
Positions and Thermal Parameters (Standard Deviations Are Given in Parentheses)

Atom	Site	sof[a]	x	y	z	$B_{eq,iso}$ (Å^2)
La(1)	8(r)	1	0.29008(4)	0.29008(4)	0.26214(6)	0.97(1)
Ti(1)	1(a)	1	0	0	0	0.74(4)
Ti(2)	4(m)	1	0.2052(2)	0	$\frac{1}{2}$	0.94(2)
Ti(3)	2(e)	1	$\frac{1}{2}$	0	$\frac{1}{2}$	0.82(3)
Ti(4)	1(c)	1	$\frac{1}{2}$	$\frac{1}{2}$	0	2.43(6)
Ti(5)	4(l)	0.5	0.4432(5)	0	0	1.07(5)
S(1)	4(o)	1	$\frac{1}{2}$	0.2354(3)	$\frac{1}{2}$	0.82(4)[b]
S(2)	2(h)	1	$\frac{1}{2}$	$\frac{1}{2}$	0.2743(5)	0.92(6)[b]
S(3)	2(g)	1	0	0	0.3174(5)	0.91(6)[b]
S(4)	8(s)	1	0.3438(2)	0	0.7188(3)	1.06(3)[b]
S(5)	4(n)	1	$\frac{1}{2}$	0.7400(3)	0	1.21(5)[b]
S(6)	8(p)	0.5	0.1753(5)	0.1525(5)	0	1.32(7)[b]
O(1)	4(k)	1	0.1875(6)	0.1875(6)	$\frac{1}{2}$	0.98(13)[b]

[a]Site occupancy factor.
[b]B_{iso}.

As no systematic absences were detected, the SHELX program was used to select from among the eight possible space groups the two most probable ones ($P4/m$ and $P4/mmm$), which we tested. The structure was initially determined in $P4/m$ (No. 83) but the atomic positions were consistent with $P4/mmm$ (No. 123). After the data for this space group were averaged, 924 independent reflections remained with $R_{int} = 0.024$. The structure was then refined by full-matrix least-squares techniques to minimize $\sum w(|F_o| - |F_c|)^2$ (with $w = 4F_o^2/[\sigma(I)^2 + (0.01F_o^2)^2]$). The position for the heavy atom (La) was found by direct methods with the program SHELX (5). The atomic positions of Ti, S, and O were determined from subsequent difference Fourier calculations. The first refinement included Ti(5) at ($\frac{1}{2}$, 0, 0) and S(6) on a site 4(j), i.e., (0.164, 0.164, 0). Thus, refinement converged to values of $R = 0.098$ and $R_w = 0.116$ and values of B_{iso} of 13.92 and 2.06 Å^2 for Ti(5) and S(6), respectively. A difference Fourier map showed a peak at (0.445, 0, 0) close to Ti(5). In a first step, we changed the special position 2(f) for Ti(5) to a more general one, 4(l), with an occupancy of 50% and obtained $R = 0.057$, $R_w = 0.060$, and $B_{iso} = 0.975$ Å^2 for Ti(5). In the

TABLE 3
Anisotropic Temperature Factors of La and Ti Atoms

	$\beta(1,1)$	$\beta(2,2)$	$\beta(3,3)$	$\beta(1,2)$	$\beta(1,3)$	$\beta(2,3)$
La(1)	0.00221(3)	0.00221(3)	0.00353(6)	−0.00010(3)	0.00027(3)	0.00027(3)
Ti(1)	0.0016(2)	0.0016(2)	0.0028(5)	0	0	0
Ti(2)	0.0015(2)	0.00098(15)	0.0061(3)	0	0	0
Ti(3)	0.0011(2)	0.0016(2)	0.0045(4)	0	0	0
Ti(4)	0.0073(4)	0.0073(4)	0.0035(7)	0	0	0
Ti(5)	0.0031(4)	0.0001(3)	0.0065(7)	0	0	0

TABLE 4
X-Ray Powder Diffraction Pattern: Observed and Calculated Intensities for Main Reflections[a]

hkl	d_{obs}	d_{calc}	I_{obs}	I_{calc}
200	5.217(3)	5.2111	31	50
002	4.192(2)	4.1920	5	10
102	3.891(2)	3.8892	18	18
220	3.687(2)	3.6848	32	44
300	3.4744(13)	3.4741	31	34
202	3.2665(12)	3.2663	100	97
320	2.8899(9)	2.8906	12	18
003	2.7952(8)	2.7947	4	4
222	2.7677(8)	2.7676	62	63
321	2.7323(8)	2.7328	10	7
302	2.6746(8)	2.6749	96	100
400	2.6054(7)	2.6056	42	53
410	2.5278(7)	2.5278	17	10
401	2.4885(7)	2.4882	4	3
330	2.4572(6)	2.4566	23	21
322	2.3795(6)	2.3797	58	42
420	2.3302(6)	2.3305	7	4
223	2.2269(5)	2.2267	8	7
303	2.1782(5)	2.1776	4	3
313	2.1305(5)	2.1315	3	2
332	2.1183(5)	2.1194	35	22
004	2.0956(5)	2.0960	29	36
430–500	2.0836(5)	2.0845	9	3–7
510	2.0439(4)	2.0440	6	5
422	2.0369(4)	2.0369	44	31
204	1.9444(4)	1.9446	15	9
520	1.9351(4)	1.9354	32	22
413	1.8750(4)	1.8747	2	2
432–502	1.8664(4)	1.8664	65	11–29
224	1.8212(3)	1.8219	11	8
304	1.7946(3)	1.7947	9	6
530	1.7872(3)	1.7874	11	6
314	1.7686(3)	1.7686	3	3
522	1.7571(3)	1.7571	21	15
600	1.7370(3)	1.7370	7	5
324	1.6967(3)	1.6969	12	9
433–503	1.6708(3)	1.6709	4	2–1
532	1.6441(3)	1.6442	6	5
540	1.6282(3)	1.6277	4	5
414	1.6134(3)	1.6135	7	4
334	1.5947(3)	1.5945	9	6
424	1.5583(2)	1.5584	3	2
622	1.5338(2)	1.5337	4	3
542	1.5172(2)	1.5173	11	9
305	1.5098(2)	1.5101	2	3
700	1.4890(2)	1.4889	6	5
434–504	1.4781(2)	1.4780	10	1–5
325	1.4505(2)	1.4504	5	2
720	1.4317(2)	1.4316	13	9
524	1.4219(2)	1.4219	16	12
405	1.4101(2)	1.4100	4	2
543	1.4065(2)	1.4065	2	2
702	1.4031(2)	1.4030	11	8
552–712	1.3905(2)	1.3905	6	5–1
444	1.3840(2)	1.3838	6	4
730	1.3686(2)	1.3685	5	3
534	1.3600(2)	1.3600	12	5
722	1.3548(2)	1.3548	21	15
206	1.3499(2)	1.3497	7	6

[a]Calculated intensities were not corrected for absorption effects.

same way, we changed the 4(*j*) position for S(6) to 8(*p*) with an occupancy of 50% and obtained $R = 0.054$, $R_w = 0.056$, and $B_{iso} = 1.32$ Å^2 for S(6). Then anisotropic temperature factors for La and Ti atoms were refined. Isotropic thermal parameters for the other atoms were kept. The final cycle of refinement resulted in values of $R = 0.045$ and $R_w = 0.048$. The final difference Fourier map possessed one residual peak within 0.64 Å of the Ti(5) atom (2% that of a La atom); the remainder of the map was essentially featureless.

The fractional coordinates and temperature factors (B_{eq} and B_{iso}) of all atoms together with their estimated standard deviations are given in Table 2. Anisotropic temperature factors of La and Ti atoms are reported in Table 3.

The powder X-ray diffraction pattern was calculated (9) using atomic positions given in Table 2. It shows a very good agreement between observed and calculated intensities (Table 4).

STRUCTURE DESCRIPTION

The structure shows one type of La polyhedron and six distinct Ti octahedra. This structure can be simply described on the basis of two kinds of layers stacked along the $\vec{c}$ axis. The first one ($z = \frac{1}{2}$) is built of two interconnected rutile-like chains of the infinite Ti(2), Ti(3), Ti(2) atom sequence in both the $\vec{a}$ and $\vec{b}$ directions. At the crossover of the chains, four Ti(2)-centered octahedra share faces (S(3), S(3), O(1)) to form a square cluster (Fig. 2). The second layer ($z = 0$) is formed by Ti(1), Ti(4) octahedra and a Ti(5) polyhedron (Fig. 3). The Ti(1)-centered octahedra connect the two layers (Fig. 4). One can see that the Ti(1)-centered octahedron joins the center of the square cluster by a corner (S(3)). We also see in Fig. 5 that six nearest sulfur atoms (four S(4) and two S(5))

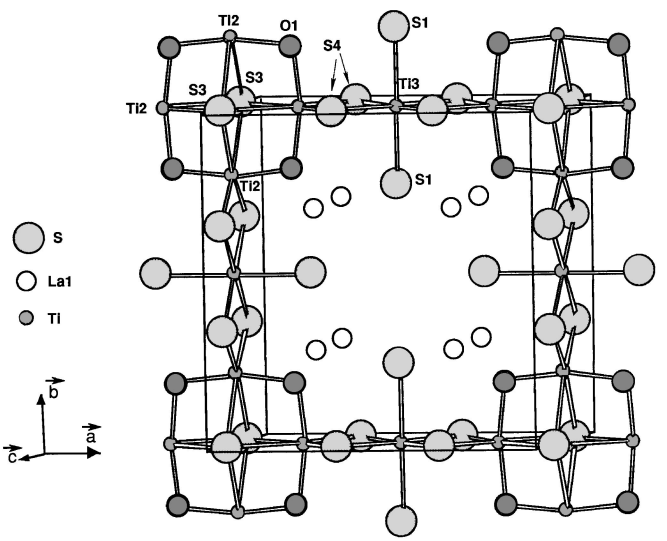

FIG. 2. Layer of Ti(2)- and Ti(3)-centered octahedra at $z = \frac{1}{2}$.

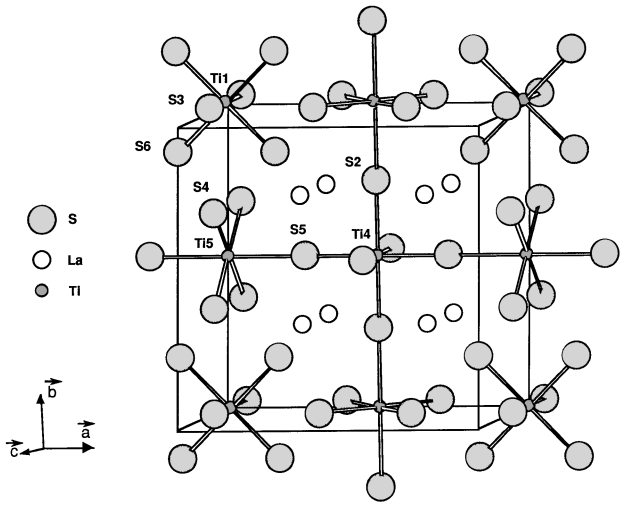

FIG. 3. Layer of Ti(1)-, Ti(4)-, and Ti(5)-centered octahedra at $z = 0$.

around Ti(5) form an octahedral surrounding. However, if atom Ti(5) was in the center of this octahedron ($x = \frac{1}{2}$), unreasonably long Ti–S distances (Ti(5)–S(4) $\approx$ 2.863 Å) would result. The refined Ti(5) position was split along the ***a*** direction to achieve a severely distorted tetrahedral coordination (inside an octahedron of S atoms), resulting in a smaller Ti(5)–S(4) distance (2.566 Å). A statistical distribution over two Ti(5) sites is assumed, which seems reasonable structurally. Such a split position for a Ti atom has already

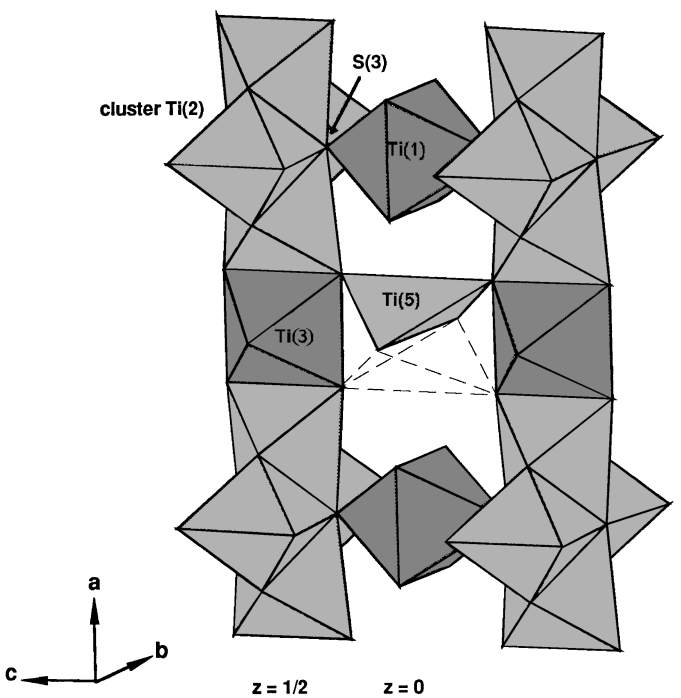

FIG. 4. Stacking of the two kinds of layers along the $\vec{c}$ axis.

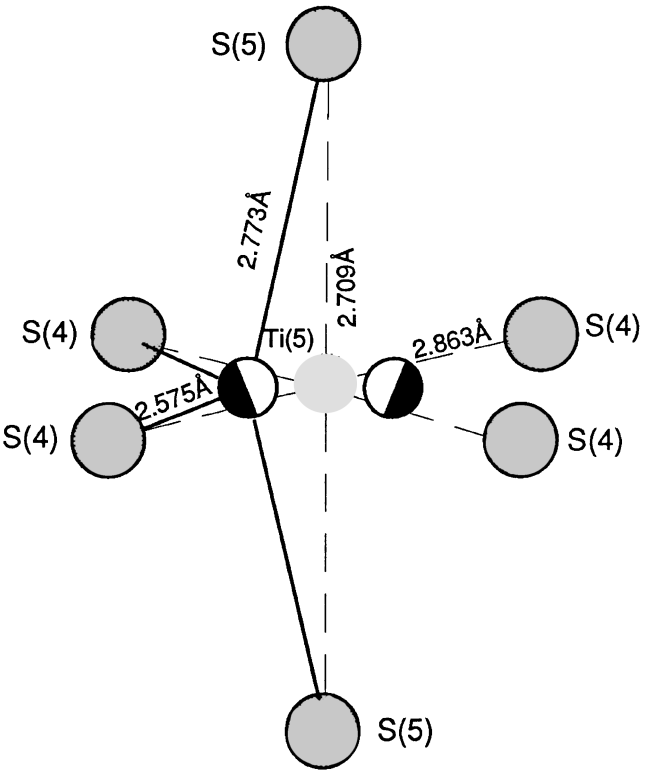

FIG. 5. Detailed environment around Ti(5) showing the shift of the position.

been described for $La_4Ti_3S_4O_8$ by Cody and Ibers (1) and for oxysulfides and oxyselenides in sheets by Guittard *et al.* (10). At the center of the layer at $z = 0$ a Ti(4) octahedron is formed by sharing corner S(5) with the Ti(5)-centered

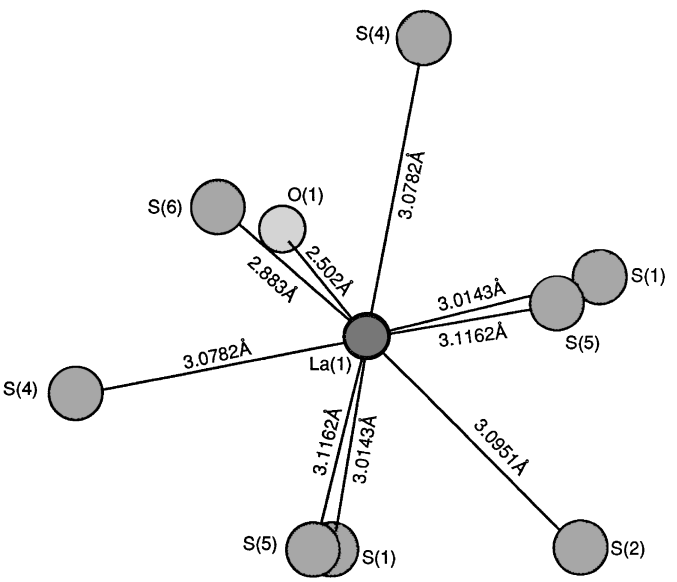

FIG. 6. Surrounding of the La atom (tricapped prism).

TABLE 5
Interatomic Distances (Å) (Standard Deviations Are Given in Parentheses)

La(1)–O(1)	2.502(4)	Ti(3)–2S(1)	2.453(3)
La(1)–2S(1)	3.0143(7)	Ti(3)–4S(4)	2.452(2)
La(1)–S(2)	3.0951(4)	$(Ti(3)–S)_{average}$	2.452
La(1)–2S(4)	3.0782(5)		
La(1)–2S(5)	3.1162(5)	Ti(4)–2S(2)	2.300(4)
La(1)–S(6)	2.883(3)	Ti(4)–4S(5)	2.500(3)
$(La(1)–S)_{average}$	3.049	$(Ti(4)–S)_{average}$	2.433
Ti(1)–2S(3)	2.661(4)	Ti(5)–2S(4)	2.575(3)
Ti(1)–4S(6)	2.421(5)	Ti(5)–2S(5)	2.774(4)
$(Ti(1)–S)_{average}$	2.501	$(Ti(5)–S)_{average}$	2.674
Ti(2)–2O(1)	1.963(6)		
Ti(2)–2S(3)	2.630(3)	Ti(2)–Ti(2)	3.025(2)
Ti(2)–2S(4)	2.334(3)	Ti2–Ti(3)	3.071(2)
$(Ti(2)–S)_{average}$	2.482		

octahedra. One can notice that the thermal parameter of Ti(4) is large. The stacking of these two kinds of layers forms tunnels in which La atoms are found in tricapped trigonal prisms (Fig. 6). Bond distances are presented in Table 5.

DISCUSSION AND CONCLUDING REMARKS

From a charge equilibrium point of view, and considering the chemical composition, two Ti^{4+} and eight Ti^{3+} should be present. However, the location of the species is not obvious. A few hypotheses can be put forward according to the mode of association of the polyhedra (face sharing, edge sharing, and corner sharing), the nature of the metal neighbors and the corresponding distances, and the distortion of certain sites.

The Ti(2) positions can be reasonably attributed to Ti^{3+} cations. Indeed, in the cluster of four face-sharing octahedra, Ti^{3+} is preferred for a better minimization of metal–metal repulsions. The observed Ti(2)–Ti(2) distance within the cluster (3.025 Å) is on the order of the critical distance (3.02 Å) for the Ti–Ti interaction (11).

The present structure is closely related to that of $La_{20}Ti_{11}S_{44}O_6$, where rutile chains containing one and two octahedra were found between similar angular clusters. Here we have only one octahedron between the clusters. Other members with longer rutile-type chains are very likely.

In Magneli phases rutile blocks are connected via shear planes involving Ti^{3+}-centered octahedra sharing faces. By analogy, we have here in a lower dimension rutile chains interrupted by Ti^{3+} octahedra sharing faces and constituting what we have already called a shear knot (2). For this reason it is very likely that Ti in the rutile chains (reduced here to one Ti(3) octahedron) is in the 4+ oxidation state. Consequently, all the other Ti would be in the Ti^{3+} state.

REFERENCES

1. J. A. Cody and J. A. Ibers, *J. Solid State Chem.* **114,** 406–412 (1995).
2. C. Deudon, A. Meerschaut, L. Cario, and J. Rouxel, *J. Solid State Chem.* **120,** 164–169 (1995).
3. L. J. Tranchitella, J. C. Fettinger, and B. W. Eichhorn, *Chem. Mater.* **8,** 2265–2271 (1996).
4. P. G. T. microanalyzer operating system mounted on the JEOL JSM 5800 LV scanning electronic microscope.
5. G. M. Sheldrick, SHELXTL V5, Siemens Analytical Instrumentation Inc., Madison, WI, 1996.
6. V. Petriceck, "JANA96: Programs for modulated and composite crystals," Institute of Physics, PRAHA, Czech Republic, 1996.
7. A. van der Lee, Institut des Matériaux de Nantes, France, 1993.
8. S. R. Hall, H. D. Flack, and J. M. Stewart, Eds., "XTAL34 Reference Manual," Universities of Western Australia, Geneva, and Maryland, 1993.
9. W. Kraus and G. Nolze, *J. Appl. Crystallogr.* **29,** 301–303 (1996).
10. M. Guittard, S. Benazeth, J. Dugué, S. Jaulmes, M. Palazzi, P. Laruelle, and J. Flahaut, *J. Solid State Chem.* **51,** 227–238 (1984).
11. J. B. Goodenough, "Les Oxydes de Métaux de Transition," p. 189. Gauthier-Villars, Montrouge, France, 1973.